# On the numerical simulation of multiphase water flows with changes of phase and strong gradients using the Homogeneous Equilibrium Model

Florian De Vuyst[1,2], Jean-Michel Ghidaglia[2] and Gérard Le Coq[2,3]

September 2002

e-mail: devuyst@mas.ecp.fr, jmg@cmla.ens-cachan.fr, glc@cmla.ens-cachan.fr

**Abstract**

We introduce a global method based on a variant of the Flux Characteristic method described by Ghidaglia *et al* [23] and designed to simulate two-phase flows. As an example, we use a three equations model with hypotheses of local thermodynamic equilibrium. Here our purpose is to qualify the Finite Volume method of regions where one can find strong gradient of density and free boundary phase transitions. We here consider a complex flow inside an injector-condenser device. The analysis will lead to a variant of the Flux Characteristic method with regularized matrix-valued sign functions. Other applications like water boiling into a hot channel and a fall of pressure in a crack due to friction will be also considered.

KEYWORDS. - Flux Characteristic Methods, two-phase flows, injector-condenser, phase transition, numerical methods, numerical analysis

AMS CLASSIFICATION. - 35L65, 65M06, 65M12, 65Z05, 76M12, 76N15, 76T10.

[1]Université de Cergy-Pontoise, BP 222 Pontoise, 95302 Cergy-Pontoise cedex, France

[2]CMLA, Ecole Normale supérieure de Cachan, CNRS UMR-8536, 61 avenue du Président Wilson, 94235 Cachan cedex, France

[3]Electricité de France, DRD/RNE, 6 quai Watier, 78401 Châtou, France

# Contents

# 1 Introduction and objectives of the present work

## 1.1 Presentation of the injector-condenser

Among the two phase flows that are analyzed by thermal-hydraulics, it is known that those with phase changes are particularly difficult to simulate numerically. Here, our goal is to perform numerical simulation tools able to enlighten and analyze the fluid flow inside an injector-condenser. This device involves complex internal energy exchanges with strong gradients of density zones and chocking (strong condensation) phenomemon. More, at our knowledge, no satisfactory numerical simulation of the steady flow in the complete injector-condenser has been presented yet. Let us mention Deberne's works [11] who obtained numerical results in agreement with experiments inside the converging nozzle up to the neck.

Our methodology is the following one : we decide to start our numerical investigation on a classical numerical method already qualified on conventional Computational Fluid Dynamics (CFD): we choose the so-called Characteristic Flux Finite Volume (CFFV) method [23],[24] with generic numerical flux

$$\Phi(U,V) = \frac{F(U)+F(V)}{2} - \frac{1}{2}\,\mathrm{sgn}(A(U,V))(F(V)-F(U))$$

where sgn denotes the scalar operator extension to diagonalizable matrices, and $A(U,V)$ denotes a mean $\mathbb{R}$-diagonalizable matrix depending on states $U$ and $V$ with pure consistency criterion $A(U,U) = D_U F(U)$. It has the advantage to give a generic upwind method and does not require some Roe matrix, shock or rarefaction waves computation. As a starting point, we choose the "simple" Homogeneous Equilibrium Model (HEM). From numerical experiments where flashing and chocking phenomenons are present, we will attempt to identify a set of numerical difficulties, analyze them for deriving a well adapted and qualified scheme, at least in the HEM context. Finally, the part of the real engine where the HEM hypotheses are almost valid will be simulated. Some numerical results will be compared to experimental ones for validation and concluding remarks.

# 2 Description and interest of the injector-condenser device

The injector is a mechanical instrument that is used for drawing along some liquid by using the driving force of another fluid (a gas or fluid). The injector-condenser is a more complex device that has been discovered at the end of the 19th century. Although it has been used for a long time in the industry, the identification of all the involved physical aspects is one of the preoccupations of the current research in two-phase flows modelling. This study is motivated by the increasing interest of *Electricité de France* (EDF) for such devices that can be a good alternative to replacing compressors in circuits of nuclear power station or can be used for additional secure devices. An experimental test bed has been implemented at *Institut National de sciences Appliquées* INSA Lyon FRANCE in 1997-99 (see Deberne [11]). It is also used for experimental reference and computational comparison. Deberne shows the principle

of working of the device, especially the range of working in the phase plane (entrance mass flux - outlet pressure). The INSA team has also identified the good level of description of two-phase flows and qualified the physical model from the experimental measures.
A simplified presentation of the injector-condensor is given on figure 1. A liquid jet of wa-

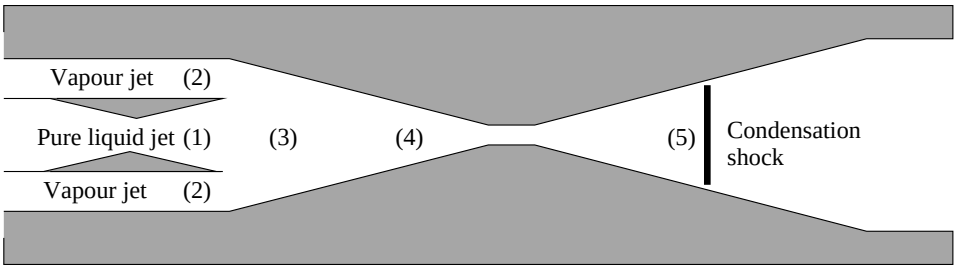


Figure 1: Injector-condenser device

ter (1) is driven by a faster jet of steam (2). The strong relative velocity between the two phases induces the spraying of liquid that becomes vaporized and is accompanied by a fall of pressure; this is the driving effect of the device. It involves complex processes of mass and energy transfer between the two phases and acts until the total relaxation to homogeneous velocities and local thermodynamic equilibrium conditions. The mixture gradually becomes homogeneous in the admittance chamber (3) and the conditions of thermodynamic equilibrium are observed to be almost reached at the end of the converging part of the nozzle (4). We then assist to a rapid condensation in the diverging part (5) into pure liquid or almost pure liquid. The energy transfer in the condensation front shows a raise of pressure that can be greater than the inlet pressure. Therefore, the injector-condenser can act as compressor. The front can be considered as a steady shock wave in the case of the HEM model that assumes an instantaneous relaxation at local thermodynamic equilibrium conditions. The jump Rankine-Hugoniot conditions for a steady shock reflect a flow evolution that passes from an upstream supersonic one to a subsonic state. The flow strongly slows down with a transfer kinetic energy - internal energy. The possible change of phase (from a two-phase mixture to pure liquid) can generate strong discontinuities of the speed of sound, typically from a few meters per second to 1500 $ms^{-1}$ and it makes its assessment still more difficult.

## 2.1 Compatibility between involved physics and HEM description

The HEM level of description is not sufficient to simulate all the device because of effects of mass and heat transfer between phases in the admittance chamber. The simulation of the whole device should involve a "six equations" model. Conversely, a difficult work of modeling of the source terms has to be done in this case. This matter is the core of Deberne's work [11]. Note also that the nonconservative products in the system of PDE have no sense although discontinous solutions can appear due to nonlinear effects. The Research team at INSA and engineers from EDF have informed us of their difficulty to capture the condensation phenomenon when using a six equations model with several industrial codes. On the contrary,

they have obtained an unexpected effect of reflashing in the diverging part, even though all the quantities correctly evolve from the mixing chamber up to the neck of the nozzle.

# 3 Classical CFD experience versus the two-phase context

The 25 years old Computational Fluid Dynamic (CFD) experience can enlighten us for good directions of investigation in the two-phase context.

## 3.1 Numerical difficulties

Since 1980, large efforts of numerical modeling of compressible flows have been developed. Although Reasearch performed important advances for the compressible Euler equations, a "ultimate scheme" (terminology used by van Leer [57]) still does not exist. Actually, the formulation of a large family of efficient conservative schemes (Osher and Solomon [39], kinetic schemes ([5] for recent works on this subject), HUS [9]) intrinsically depend of the structure of continuous or discontinuous waves of approximate Riemann problems, that make then inoperable in the two-phase context because of the too complex structure of Riemann problem solutions. Then the panel of usable methods becomes more tight. The Roe scheme [44] can be used in some cases of multiphase models, but the numerical flux stays not generic and hard work has to be done for the computation of the Roe matrices. More, this work need to be repeated each time the physical model is modified or changed. Today, Roe scheme is still the most employed scheme for two phase applications. Note that recently, Liou extended his AUSM+ scheme to six equations two-phase models [36] and has obtained good results. In this paper, we rather use most generic methods for model independence purposes. The so-called Characteristic Flux Finite Volume schemes (CFFV, [23],[24]) have the advantage to fulfil this feature. As a starting point, we propose to explore the behavior of CFFV for the injector-condenser problem.

It is also interesting to note that the philosophy of CFD and two-phase worlds can be sometimes divergent. The papers "Towards the ultimate scheme.." written by van Leer ([57] reveal investigation for achieving both stability, robustness and accuracy. In two phase flows, the sense "Towards the ultimate scheme.." is ambiguous. Indeed, it is known that systems of PDEs from two-phase modelling are conditionally hyperbolic. Then numerical schemes need to be dissipative enough to produce stable oscillation free discrete solutions. This is in opposition the usual expectation of accuracy of the numerical scheme. That is why we will not talk about high order of accuracy in this paper.

## 3.2 Difficulties due to underlying Physics

Gas dynamics modeling is essentially well-closed, except for particular contexts except when very complex physical phenomena need to be taken into account : chemistry, ionization thermal radiation and plasma coupling for hypersonic flows [37], or compressible turbulence [12], etc. Moreover, equations of state have often a closed form (although possibly implicit) and propagation velocities are well-defined and explicitly determined. Equations are mostly in

conservation form. More, a good modeling generally gives entropy-flux pairs that state the well-posedness and the stability of the systems, giving criteria for weak distribution solutions selection. The physical flux is often smooth ($\mathcal{C}^1$) which implies a smooth evolution of derivative-based quantities like the speed of sound. Models do not involve free boundaries (except for fluid-structure interaction problems that are difficult problems).

In two-phase water flows, there exists some fundamental reasons not to have a universally approved closure because of the lack of knowledge concerning some microscopic phenomena (*e.g.* nucleation of bubbles at a wall) and because of some averaging process that make loose some properties : hyperbolicity, etc. More, it is not clear to give a sense to a averaged speed of sound in a mixture of liquid and steam. For the so-called five or six equation models, the equations make appear nonconservative terms that have not a rigorous sense for discontinuous weak solutions. Because the equations are often formulated in such a way that local conditions of thermal equilibrium are not supposed, it cannot be found some entropy-flux pairs. Finally, for equilibrium models, phase transitions produce a strong jump of speed of sound. That means that the physical flux is not of class $\mathcal{C}^1$, but only Lipschitz continuous. This lack of regularity can be a source of numerical difficulty especially when implicit schemes and fixed point methods are used. More, the Homogenous Equilibrium Model (HEM) can lead to aberrant values of Mach-like numbers (up to 100!). It is also classical in the two-phase world to meet strong (subsonic - supersonic) transition inducing a jump of number of left and right characteristics. For example, for pressure and temperature respectively close to 1 bar and 100 degrees Celcius, the speed of sound can jump from about 1500 $ms^{-1}$ to 5 $ms^{-1}$ in the water. This is the case for a boiling water into a hot channel (see the end of the paper for simulations). On the other hand, because of the presence of large speed of sound in pure liquid, flow regions of very low mach number are often present. It is then expected to encounter well-known problems of low Mach number already encountered in CFD (low convergence to steady state, lack of accuracy, ...).

### 3.3 Direction of investigation

All these difficulties lead us to adopt the following strategy:

(i) begin with the simplest physical model (possibly with no phasic mass or energy transfer),

(ii) work with the smallest number of equations,

(iii) define equations without nonconservative terms,

(iv) study problems with one space variable...

(v) ...while make appear characteristic two-phase behaviours (phase transition, flashing, chocking),

(vi) progressively enrich the model with lowest paper and computational effort and qualify CFFV methods.

In this context, the milestone is certainly to insure the three fundamental conservations : mass, momentum and energy. To be more precise, let us consider a quasi-1D flow (see Appendix A) in a pipe (or a nozzle) with variable section $\Sigma$ and constant slip velocity $u_r$ between the two phases. The three aforementioned conservation laws read then as follows :

$$(\rho\Sigma)_t + (\rho u\Sigma)_x = 0, \tag{1}$$

$$(\rho u\Sigma)_t + \left(\Sigma\left(\rho u^2 + p + \rho C(1-C){u_r}^2\right)\right)_x = p\Sigma_x, \tag{2}$$

$$(\rho E\Sigma)_t + \left(\Sigma\left(\rho H u + \rho(L + (\frac{1}{2} - C){u_r}^2 + u u_r)C(1-C)u_r\right)\right)_x = 0\,. \tag{3}$$

In these equations, $\rho$, $u$ and $E$ denote respectively the (mean) density, the velocity and the specific total energy :

$$\rho E = \frac{1}{2}\rho u^2 + \frac{1}{2}\rho C(1-C){u_r}^2 + \rho e\,, \tag{4}$$

$p$ denotes the pressure, $C$ the quality, $H = E + \frac{p}{\rho}$ the specific total enthalpy and $L$ the latent heat.

If the three partial differential equations (1) to (3) are sufficient to describe the evolution of the flow, we have to parametrize the physical state *via* three independent variables. Actually we are going to use two thermodynamic variables and a cinematic one. For the latest, we choose, as it is usually done, the velocity $u$. Concerning the former, that will depend on whether we are dealing with a mixture $0 < C < 1$ or a pure fluid $C = 0$ (liquid) or $C = 1$ (vapor).
In the case of a pure fluid, we shall use the temperature $T$ and the pressure $p$ as independent variables, *i.e.* we consider all the quantities as functions of $(p, T, u)$. While in the case of a mixture, we shall use the temperature $T$ and the quality $C$ as independent variables, *i.e.* we express all the quantities as functions of $(C, T, u)$.

# 4 Approximation of the equation of state

Starting with a numerical value of the set of 3 conservative variables $v = (\rho\Sigma, \rho u\Sigma, \rho E\Sigma)$, we aim to compute the corresponding value of the flux $f(v)$ given by formula (13). This requires the computation of the thermodynamic variables. In the case where $u_r = 0$, as we know that $v$ immediately enables to compute $\rho$ and $e$, and then that one has to find either $T$ and $C$ or $p$ and $T$ depending on whether we are dealing with a mixture or not. This is an inverse problem which has to be solved numerically by using an iterative method (we shall use Newton's one). At each iteration, one has to compute thermodynamic variables or coefficients by using water tables. This can be very costly in terms of CPU time and therefore, we suggest a proper linearization of such tables which leads to a more efficient method without loosing the physical meaning of the equations of state (see Appendix C for the complete construction).

### 4.1 Continuity at the phase transitions

We denote by $\rho_k$, $\tau_k \equiv 1/\rho_k$, $h_k$, $e_k \equiv h_k - p_k\tau_k$ and $s_k$, the density, the specific volume, the specific enthalpy, the specific internal energy and the specific entropy of the fluid, the index $k$ being either $\ell$ for the liquid or $v$ for the vapor.
Suppose that the laws $\tau_\ell(p,T)$, $h_\ell(p,T)$, $\tau_v(p,T)$ and $h_v(p,T)$ are known. In the two-phase mixture, both the liquid and the vapour phases change at conditions of saturation. In that case, the pressure is linked to the temperature by the law of pressure of saturation $p_s$ :

$$p \;=\; p_s(T) \tag{5}$$

This function is expected to be continuously differentiable and strictly monotonous, so that we can notably invert it to get the temperature of saturation $T_s$ as function of the pressure $T \;=\; T_s(p) \;=\; (p_s)^{-1}(p)$. So we can respectively define the specific volume and enthalpy of saturation by

$$\tau_{k;s}(T) \;=\; \tau_k(p_s(T),T), \tag{6}$$
$$h_{k;s}(T) \;=\; h_k(p_s(T),T) \tag{7}$$

where the subscript $k$ equals to $l$ or $v$. Finally, we define some average quantities $\tau$ and $h$ to define the mixture. The quality $C$, $0 \le C \le 1$ infers on the extensive variables $\tau$ and $h$. The pair $(C,T)$ is defined as the unique solution in $[0,1]\times]0,+\infty[$ of

$$\tau \;=\; C\;\tau_{v;s}(T) + (1-C)\tau_{l;s}(T), \tag{8}$$

$$h \;=\; C\;h_{v;s}(T) + (1-C)h_{l;s}(T). \tag{9}$$

Consequently, variables $C$ and $T$ play the role of free thermodynamic variables in the mixture.

### 4.2 Approximation of the convection operator via flux schemes

The system (1) to (3) can be written as :

$$\frac{\partial U}{\partial t} + \frac{\partial F(U)}{\partial x} = S(U)\,, \tag{10}$$

with

$$U = (\rho\Sigma, \rho u\Sigma, \rho E\Sigma)\,, \tag{11}$$
$$S(U) = (0, p\Sigma_x, 0)\,, \tag{12}$$
$$F(U) = (F_1(U), F_2(U), F_3(U))\,, \tag{13}$$
$$F_1(U) = \rho u\Sigma,$$
$$F_2(U) = \left(\rho u^2 + p + \rho C(1-C){u_r}^2\right)\Sigma\,,$$
$$F_3(U) = \left(\rho H u + \rho(L + (\frac{1}{2} - C){u_r}^2 + u u_r)C(1-C)u_r\right)\Sigma.$$

We denote by $A(U)$ the Jacobian matrix $\frac{\partial F(U)}{\partial U}$ and we assume that the three characteristic velocities are distinct *i.e.* $\Delta > 0$. Hence (10) is *regularly hyperbolic* that is to say: for every $U$ there exists a smooth basis $(r_1(U), r_2(U), r_3(U))$ of $\mathbb{R}^3$ made of eigenvectors of $A(U)$ : $\exists \lambda_k(U) \in \mathbb{R}$ such that $A(U)r_k(U) = \lambda_k(U)r_k(U)$. It is then possible to construct a $(l_1(U), l_2(U), l_3(U))$ such that ${}^tA(U)l_k(U) = \lambda_k(U)l_k(U)$ and $l_k(U) \cdot r_p(U) = \delta_{k,p}$.
Let $\mathbb{R} = \cup_{j\in\mathbb{Z}}[x_{j-1/2}, x_{j+1/2}]$ be a one dimensional mesh. Our goal is to discretize (10) by a finite volume method. We look for an approximation $U_j^n$ of $\frac{1}{\Delta x_j \Delta t_n}\int_{x_{j-1/2}}^{x_{j+1/2}}\int_{t_{n+1}}^{t_n} U(x,t)\,dx\,dt$, $\Delta x_j \equiv x_{j+1/2} - x_{j-1/2}$, $\Delta t_n \equiv t_{n+1} - t_n$ (we also have $\mathbb{R}_+ = \cup_{n\in\mathbb{N}}[t_n, t_{n+1}]$). The discretization of (10) according to the implicit Characteristic Flux Method (Ghidaglia, Kumbaro and Le Coq [23],[24]) reads as :

$$U_j^{n+1} = U_j^n - \frac{\Delta t_n}{\Delta x_j}\left(U_{j+1/2}^{n+1} - U_{j-1/2}^{n+1}\right) + S_j^{n+1}\,, \tag{14}$$

About the important question of the numerical treatment of the source terms (computation of $S_j^{n+1}$), we use the same upwind strategy as exposed in Alouges *et al* [1]. The implicit characteristic flux $F_{j+1/2}^{n+1}$ is obtained by the following formula

$$F_{j+1/2}^{n+1} = G_{j+1/2}^{CF}(U_j^n, U_{j+1}^n; F(U_j^{n+1}), F(U_{j+1}^{n+1}))\,, \tag{15}$$

and

$$G_{j+1/2}^{CF}(U, V; F, G) \equiv \frac{F+G}{2} - B(\mu_{j+1/2}; U, V)\frac{G-F}{2}\,, \tag{16}$$

where $\mu_{j+1/2}$ is a mean value between the two states $U$ and $V$ which depends also on $\Delta x_j$ and $\Delta x_{j+1}$ and $B(\mu; U, V)$ is the sign of the matrix $A(\mu)$ :

$$B(\mu; U, V)\Phi = \sum_{k=1}^{3} \mathrm{sgn}(\lambda_k(\mu))(l_k(\mu)\cdot\Phi)r_k(\mu)\,. \tag{17}$$

In this last formula, since $\mathrm{sgn}(\lambda) = -1$ or $1$, one could reproach a lack of regularity of this numerical flux in some particularly stiff instances. This feature occurs for example at phase transitions between the pure liquid and the two-phase mixture. Because the eigenvalues are computed using an averaged state $\mu$, we have to decide whether this mean state is liquid or corresponds to a mixture. In both cases, one favours one state rather than another one. More, because the scheme is implicit, an iterative fixed point method like Newton's one is used to solve the resulting nonlinear system of equations to solve a teach time steps. Because the flux is not differentiable at transition, emerging numerical spurious oscillations (sensible on pressure profile) have been observed during iterations that can make the computation unstable.
To bring some regularity on the numerical flux, we propose in the next section a smoother family of numerical fluxes that does not strictly fall into the family of characteristic fluxes, but can approach them as close as wanted *via* a regularization parameter $\epsilon$. This is equivalent to a regularization of the *sign* functions. The truncated numerical dissipation due to regularization is compensated by an additional term of the form

$$-Q_\epsilon(\mu_{j+1/2}; U, V)\,\frac{V-U}{2}$$

for a particular dissipation matrix $Q_\epsilon \geq 0$ that vanishes when $\epsilon \to 0$.

# 5 A new class of upwind scheme involving regularized sign functions

## 5.1 First step

We are looking for the "best" local interpolation inside two adjacent cells $I$ and $J$ of respective constant state $U$ and $V$. For the sake of simplicity, suppose that $|I| = |J| = h$. Given a first order numerical flux, the interpolation must respect the upwinding feature. We still work on a hyperbolic system of conservation laws

$$\partial_t U + \partial_x F(U) = 0,\ U, F(U) \in \mathbb{R}^p$$

The interpolation is supposed piecewise linear per cell with possible discontinuity at interface. We then define two interpolation states at interface:

$$\tilde{U} \ = \ U + \frac{1}{2} S_U (V - U),\ \tilde{V} \ = \ V - \frac{1}{2} S_V (V - U), \tag{18}$$

where $S_U$, $S_V \in \mathcal{M}_p(\mathbb{R})$. The construction of such matrices is detailed later. At the moment, let $A(U, V)$ be a matrix that satisfies both consistency and decomposition conditions:

$$\begin{array}{l} A(U,V) \text{ is diagonalizable in } \mathbb{R}, \\ A(U,U) \ = \ D_U F(U). \end{array} \tag{19}$$

We denote by $(\lambda_k)_{k=1,p}$ the eigenvalues of $A(U, V)$ and $R$ the matrix of right eigenvectors arranged in column, so we have the decomposition

$$A \ = \ R \, \mathrm{diag}\,(\lambda_k)\, R^{-1}.$$

The matrices $S_U$ and $S_V$ can be more precisely detailed. We equip these matrices of family of slope parameters $(s_{k;U})_{k=1,p}$ and $(s_{k;V})_{k=1,p}$ estimated in the basis of eigenvectors, that means

$$S_U \ = \ R \, \mathrm{diag}\,(s_{k;U})\, R^{-1},\ S_V \ = \ R \, \mathrm{diag}\,(s_{k;V})\, R^{-1}. \tag{20}$$

Finally, let $q \in [0, 1]$. We consider a family of upwind numerical fluxes $(q, s_{k;U}, s_{k;V})$ of the form

$$\Phi(U, V) \ = \ \frac{F(\tilde{U}) + F(\tilde{V})}{2} - \frac{1}{2}\, q \, |A(U, V)| \, (\tilde{V} - \tilde{U}).$$

We are going to characterize necessary and sufficient conditions on $(q, s_{k;U}, s_{k;V})$ to have a smooth (locally Lipschitz continuous) and upwind numerical flux.

**Monotonicity criteria.**

**Proposition 1** *The condition of monotony property for the local interpolation is*

$$0 \ \leq \ s_{k;U} \ \leq \ 2, \ \ 0 \ \leq \ s_{k;V} \ \leq \ 2. \tag{21}$$

Remark that the case $S_U = S_V = I$ gives a second order interpolation.

**Upwinding and continuity criteria**

**Proposition 2** *1. The conditions for upwind process are*

$$-\,q\,\frac{s_{k;U}+s_{k;V}}{2}\;+\;\mathrm{sgn}(\lambda_k)\,\frac{s_{k;V}-s_{k;U}}{2}\geq\;1-q\qquad\forall k\in\{1...p\},\tag{22}$$

*2. The only admissible value of $q$ for continuous coefficients $\alpha_k$ at sonic points $\lambda_k = 0$ is $q = 1$.*

**Proof.** We expose the proof in the linear case $F(U) = A\,U$ for constant matrix $A$. We write the explicit difference scheme of initial state $V$ in the left half of the cell J at the right of the interface $(I, J)$:

$$\begin{aligned}V^{n+1}\;&=\;V-2\mu_n\left\{AV-\frac{1}{2}A\,(V+U)+\frac{1}{2}R\,\mathrm{diag}\left(\lambda_k\,\frac{s_{k;U}+s_{k;V}}{2}\right)R^{-1}(V-U)\right.\\&+\;\left.\frac{1}{2}\,q\,|A|\,R\,\mathrm{diag}\left(1-\frac{s_{k;U}+s_{k;V}}{2}\right)R^{-1}(V-U)\right\},\end{aligned}$$

where $\mu_n = \Delta t_n/h$. The expression can be written again

$$V^{n+1}\;=\;V-2\mu^n\;R\,\mathrm{diag}\left(\frac{1}{2}\lambda_k+\frac{1}{2}q\,|\lambda_k|\,(1-\frac{s_{k;U}+s_{k;V}}{2})+\frac{1}{2}\lambda_k\frac{s_{k;V}-s_{k;U}}{2}\right)R^{-1}\;(V-U).$$

The scheme is expected to be upwind. We want to only capture the positive propagation velocities in the half celle, so that we are looking for coefficients such that

$$\frac{1}{2}\lambda_k+\frac{1}{2}q\,|\lambda_k|\,(1-\frac{s_{k;U}+s_{k;V}}{2})+\frac{1}{2}\lambda_k\frac{s_{k;V}-s_{k;U}}{2}\;\geq\;0$$

is true for all $k$. This gives

$$\frac{1-q}{2}\,s_{k;V}\;-\;\frac{1+q}{2}\,s_{k;U}\geq\;-1-q$$

for $\lambda_k \geq 0$ and

$$-\frac{1-q}{2}\,s_{k;U}\;+\;\frac{1+q}{2}\,s_{k;V}\leq -1+q$$

for $\lambda_k \leq 0$. In the same way, the scheme in the left half celle of initial state $U$ gives

$$U^{n+1}\;=\;U-2\mu^n\;R\,\mathrm{diag}\left(-\frac{1}{2}\lambda_k+\frac{1}{2}q\,|\lambda_k|\,(1-\frac{s_{k;U}+s_{k;V}}{2})+\frac{1}{2}\lambda_k\frac{s_{k;V}-s_{k;U}}{2}\right)R^{-1}\;(V-U)$$

with conditions

$$\frac{1-q}{2}\,s_{k;V}\;-\;\frac{1+q}{2}\,s_{k;V}\geq\;1-q$$

for $\lambda_k \geq 0$ and

$$-\frac{1-q}{2}\,s_{k;U}\;+\;\frac{1+q}{2}\,s_{k;V}\leq 1+q$$

for $\lambda_k \leq 0$. Secondly, we are looking conditions on $q$ to have continuity on coefficients at $\lambda_k = 0$. By difference one gets

$$q\,(s_{k;U} + s_{k;V}) \;=\; 2(q-1) \;\; \forall k.$$

This is only possible for $q = 1$. In that case, if $\lambda_k = 0$, we find $s_{k;U} = s_{k;V} = 0$.

**Corollary 1** *In the case $q = 1$, the admissible values for $s_{k;U}$ ad $s_{k;V}$ are*

$$\begin{array}{l} \textit{If } \lambda_k > 0, \;\; \textit{then } s_{k;U} = 0, \;\; 0 \leq s_{k;V} \leq 2, \\ \textit{if } \lambda_k < 0, \;\; \textit{then } 0 \leq s_{k;U} \leq 2, \;\; s_{k;V} = 0, \\ \textit{if } \lambda_k = 0, \;\; \textit{then } s_{k;U} = s_{k;V} = 0. \end{array}$$

## 5.2 Discussion

There exists some large degrees of freedom for the design of coefficients $s_{k;U}$ $s_{k;V}$ (see as functions of eigenvalues $\lambda_k$).
The idea here is to choose slope coefficients that are simple to calculate and give good properties. Let us first recall the expression of the numerical flux for $q = 1$:

$$\begin{array}{rcl} \Phi(U,V) & = & \dfrac{1}{2}\left\{F(U + \dfrac{1}{2}S_U(V-U)) + F(V - \dfrac{1}{2}S_V(V-U))\right\} \\ & & - \dfrac{1}{2}\left(I - \dfrac{S_U + S_V}{2}\right)|A(U,V)|\,(V-U). \end{array}$$

**1.** First, states $U$ and $V$ play the same role. The symmetry invite us to choose

$$s_{k;V}(\lambda) \;=\; s_{k;U}(-\lambda).$$

**2.** There is a priori no reason to distinguish the different fields of the system, so we propose

$$s_{k;U}(\lambda) \;=\; \chi(\lambda)$$

independent of $k$.
**3.** Function $\chi$ is supposed to be at least Lipschitz continuous. For numerical purposes, it is reasonable to design these functions as piecewise smooth.
**4.** The shape of the numerical flux shows a flux term added by a viscous term. Again for numerical reasons (accuracy), is moral to load the flux as strong as possible for physical. Indeed, suppose that all the waves produced by the interaction of the two states are positive. Then necessary, $s_{k;U} = 0\;\forall k$. Consequently, the choice $s_{k;V} = 2\;\forall k$ which is admissible makes the viscous term falling down to zero. On the other hand ($s_{k;V} = 2\;\forall k$), we get

$$\Phi(U,V) \;=\; F(U). \tag{23}$$

This is exactly the expected flux which is also the Godunov flux which satisfies discrete entropy inequalities. By this construction, this family falls into the class of upwind difference schemes this the definition given by Harten, Lax and van Leer [32].

Of course, because of the continuity constraints at $\lambda = 0$ with $s_{k;U} = 0$, this property cannot be true for values $\lambda_k$ belonging to a "small" interval $[0, \epsilon]$, $\epsilon > 0$. Up to a parameter, we can choose $\chi(\lambda) = 2\ \forall \lambda \in [\epsilon, +\infty[$. Parameter $\epsilon$ could be chosen according to the minimum distance between two consecutive waves for example. For simplicity, we suppose here that all the characteristic fields are simple, otherwise we should group all the linearly degenerate fields with same eigenvalue and the construction still holds. We resume the previous construction and remarks by the following result:

**Proposition 3** *From any admissible states $U$ and $V$, we define a mean diagonalizable matrix $A(U,V)$ that respects the consistency condition $A(U,U) = A(U)$. Let $\lambda_k(U,V)$ be the kth eigenvalue of $A(U,V)$ and $\epsilon$ a positive real number such that*

$$\epsilon \ < \ \min_k |\lambda_{k+1}(U,V) - \lambda_k(U,V)|\,. \tag{24}$$

*Let $\chi_\epsilon : \mathbb{R} \to [0,2]$ be a locally Lipschitz continuous function such that*

$$\begin{array}{rcl} \chi(x) & = & 0 \quad \forall x \geq 0, \\ \chi(x) & = & 2 \quad \forall x \leq \epsilon. \end{array} \tag{25}$$

*Then the following numerical scheme with numerical flux $\Phi(U,V)$ equal to*

$$\begin{array}{l} \dfrac{1}{2}\left\{ F(U + \dfrac{1}{2} R\,\mathrm{diag}\,(\chi_\epsilon(\lambda_k))\,R^{-1}(V-U)) + F(V - \dfrac{1}{2} R\,\mathrm{diag}\,(\chi_\epsilon(-\lambda_k))\,R^{-1}(V-U)) \right\} \\ \qquad - \ \dfrac{1}{2}\left( I - R\,\mathrm{diag}\left( \dfrac{\chi_\epsilon(\lambda_k) + \chi_\epsilon(-\lambda_k)}{2} \right) R^{-1} \right) |A(U,V)|\ (V-U). \end{array} \tag{26}$$

leads to an upwind scheme in the sense of Harten, Lax and van Leer with Lipschitz continuous flux. The stability criterion is given by

$$\mu_n \ \max_{j\in\mathbb{Z}} \max_k |\lambda_k(A(U_j, U_{j+1}))| < 1.$$

Let us remark that the flux cannot be read under a usual viscous form and that the interpolated states $U + \frac{1}{2} R\,\mathrm{diag}\,(\chi_\epsilon(\lambda_k))\,R^{-1}(V-U)$ can become not be admissible (negative density, negative energy for example). This motivates the introduction of interpolations now applied to fluxes.

### 5.3 Second step. Analysis using slopes on both states and flux

The same analysis can be performed combining both slopes on states and flux. We here more define two interpolated flux $\tilde{F}_U$ and $\tilde{F}_V$ with expressions

$$\tilde{F}_U \ = \ F(U) + \frac{1}{2}\, S_U\,(F(V) - F(U)),\ \tilde{F}_V \ = \ F(V) - \frac{1}{2}\, S_V\,(F(V) - F(U)), \tag{27}$$

sharing the same slope coefficients than the states. We are looking for a numerical flux of the form

$$\Phi(U,V) \ = \ \frac{\tilde{F}_U + \tilde{F}_V}{2} - \frac{1}{2}\, q\ |A(U,V)|\ (\tilde{V} - \tilde{U}).$$

For $q = 1$, the numerical flux has the following viscous form

$$\Phi(U,V) \;=\; \frac{F_U + F_V}{2} \;-\; \frac{1}{2}\frac{S_V - S_U}{2}\,(F(V) - F(U)) \;-\; \frac{1}{2}\left(\mathsf{I} - \frac{S_U + S_V}{2}\right)\,|A(U,V)|\;(V-U). \tag{28}$$

It is written in viscous form. More, its script is close to those of characteristic flux schemes introduced by Ghidaglia, Kumbaro and Le Coq [23],[24]. If functions $s_{k;U}$ and $s_{k;V}$ are built from a function $\chi_\epsilon$ as discussed before, it is clear to see that the odd function

$$\frac{s_{k;V} - s_{k;U}}{2} \;=\; \frac{\chi_\epsilon(-\lambda_k) - \chi_\epsilon(\lambda_k)}{2}$$

with values in $[-1,1]$ plays the role of a regularized sign function, whereas the compactly bounded support even function

$$1 - \frac{s_{k;V} + s_{k;U}}{2} \;=\; 1 - \frac{\chi_\epsilon(-\lambda_k) + \chi_\epsilon(\lambda_k)}{2}$$

with values in $[0,1]$ provides the missing numerical dissipation for strict upwinding and stability. We can finally resume:

**Proposition 4** *Under the same hypotheses than Proposition 1, the difference scheme with numerical flux*

$$\Phi(U,V) = \frac{F_U + F_V}{2} \;-\; \frac{1}{2}\,R\,\mathrm{diag}\,(\sigma_\epsilon(\lambda_k))\,R^{-1}(F(V) - F(U)) - \frac{1}{2}\,R\,\mathrm{diag}\,(\hbar_\epsilon(\lambda_k))\,R^{-1}(V-U), \tag{29}$$

*with*

$$\sigma_\epsilon(\lambda) = \frac{\chi_\epsilon(-\lambda_k) - \chi_\epsilon(\lambda_k)}{2}, \quad \hbar_\epsilon(\lambda) = 1 - \frac{\chi_\epsilon(\lambda_k) + \chi_\epsilon(-\lambda_k)}{2}$$

*has the same properties of smoothness and upwinding. The limit case $\epsilon \to 0$ gives the family of characteristic flux schemes.*

**Example of numerical flux** The simplest Lipschitz continuous flux is built using the piecewise linear function $\chi_\epsilon$

$$\chi_\epsilon(\lambda) = \begin{cases} 2 \text{ if } \lambda \le -\epsilon, \\ -\frac{2\lambda}{\epsilon} \text{ if } -\epsilon < \lambda \le 0, \\ 0 \text{ otherwise.} \end{cases} \tag{30}$$

**Proposition 5** *For the choice (30),*

$$\sigma_\epsilon(\lambda) \;=\; \begin{cases} \mathrm{sgn}(\lambda) \;\textit{if}\; |\frac{\lambda}{\epsilon}| \ge 1, \\ \frac{\lambda}{\epsilon} \;\textit{otherwise,} \end{cases} \qquad \hbar_\epsilon(\lambda) \;=\; \begin{cases} 1 - \left|\frac{\lambda}{\epsilon}\right| \;\textit{if}\; |\frac{\lambda}{\epsilon}| \le 1, \\ 0 \;\textit{otherwise.} \end{cases} \tag{31}$$

*or again under a condensed form*

$$\sigma_\epsilon(\lambda) = \min\left(1, \left|\frac{\lambda}{\epsilon}\right|\right)\,\mathrm{sgn}(\frac{\lambda}{\epsilon}),\;\; \hbar_\epsilon(\lambda) = \max\left(0, 1 - \left|\frac{\lambda}{\epsilon}\right|\right)$$

*Function $\sigma_\epsilon$ plays the role of a regularized sign function.*

Another interesting feature of the last construction is that the resulting scheme preserves stationary contact discontinuities provided additional hypotheses on $A(U,V)$ that are easy to fulfil. So it provides strong accuracy for low moving linear waves.

**Proposition 6** *Suppose more that $A(U,V)$ preserves the kth Riemann invariant $\lambda_k$ for two states $U$ and $V$ separated by a k-contact discontinuity, that means*

$$\lambda_k(A(U,V)) = \lambda_k(A(U)) = \lambda_k(A(V)),\ k \in LD(F),$$

*where $LD(F)$ is the set of indices $k \in \{1,...,p\}$ of linearly degenerate fields for flux $F$. Then the difference scheme of numerical flux (29) perfectly preserves stationary contact discontinuities.*

**Proof.** Suppose that $F(U) = F(V)$, $U \neq V$ with $\lambda_k(A(U) = \lambda_k(A(V)) = \lambda_k(A(U,V)) = 0$. So the first dissipation term in (29) is zero. Then the $k$th eigenvalue of diagonal matrix $\mathrm{diag}\,(\hbar_\epsilon(\lambda_l)|\lambda_l|)$ is zero. Otherwise, because $\epsilon$ does not exceed the distance between two eigenvalues (by hypothesis (24)) and because function $\hbar_\epsilon$ is compactly supported on the interval $[-\epsilon,\epsilon]$, then $\hbar_\epsilon(\lambda_l) = 0$ for all $l \neq k$.

This numerical flux can be straitforwardly extended to multidimensional problems using for example the property of invariance by rotation of the equations.

# 6 Application to injector-condenser flows

We present two examples of injector-condenser configuration. The first one is a "6 bar" example and has been built to validate and qualify the whole flux scheme method [23]. The model constants given by table 2 are used. The second one corresponds to a real case extracted from conditions of experiment of the INSA test bed. In this case, data from table 1 are used. Because we cannot simulate the whole device, we have extracted data from experiments at the position of converging nozzle where the homogeneous equilibirum hypothesis is almost verified. Because at this definite location the flow is supersonic, this can define the entrance of our computational domain and we can use measured data as inlet boundary conditions. In both cases, the source terms are $S_2(v) = p\frac{\partial \Sigma}{\partial x}$ that modelizes the influence of the geometry and $S_3(v) = 0$ (no heat flux).

**6 bar injector-condenser test case.** The nozzle is 1 meter long. We use 150 computational points with a uniform space step. The section $\Sigma$ is defined as

$$\Sigma(x) \ = \ \begin{cases} 1 - 0.015\left(1 - w^2(3-2w) + 15w^2(1-w)^2\right) & \text{if } 0 \leq w \leq 1, \\ 1 \text{ otherwise,} \end{cases}$$

where $w = x/0.9$. The numerical process to capture an operating mode at imposed outlet pressure ($p_s = 6.8$) bar is similar to the experimental one. First, we impose an outflow pressure lower than $p_s$, that is to say 6 bar. The entrance mass flux $\rho u \Sigma$ will be chosen small enough in order to get first a whole subsonic flow. The field is initialized with a two-phase mixture at uniform pressure $p = 6$ bar and a quality $C = 10^{-2}$. Because the flow is subsonic

at the entrance, we have to impose an additional constraint, namely on the specific enthalpy $h$ compatible with the constraints $p = 6$ bar and $C = 10^{-2}$. Secondly, we successively increase the values of inflow mass flux and outlet pressure in order to produce a supersonic region, coming with the condensation shock and to stabilize the shock in the computational domain. At fixed outlet pressure, increasing the inlet mass flux shifts the condensation to the right. At fixed inlet mass flux, increasing the outlet pressure results in shifting the shock to the left. Finally, at the end of the computation, the inflow mass flux is equal to $\rho u \Sigma = 3700$ (in SI unit). On figure 2, we sum up the strategy of priming of the injector-condenser. On

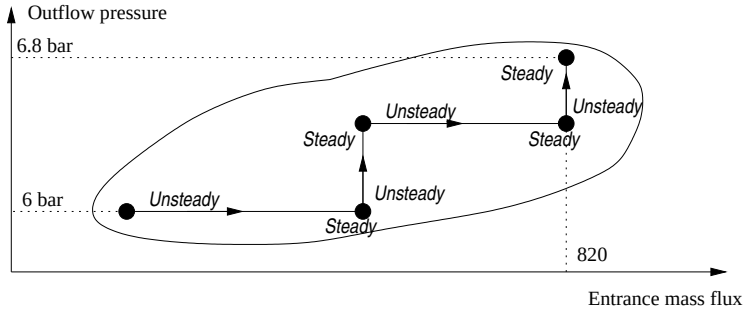


Figure 2: Strategy of computation at fixed outflow pressure 6.8 bar

figure 3, we show the nozzle section profile and the numerical steady solutions obtained at $p_s = 6.8$ bar. On a Mollier diagram, one can verify that all the thermodynamic variables evolve correctly, which validates our approximation on equations of state.
Then, the main difficulty of computation is linked to the points of phase transition, where the physical flux is not differentiable. This has the consequence to produce large oscillations during the fixed point of the nonlinear implicit method. Sometimes it happens to throw the robustness off the scent when too large CFL numbers were used. For the moment, our only alternative is to drastically reduce the CFL number, typically to one where CFL numbers up to 50000 can be used without phase transition.

**INSA test bed simulation.** This numerical test case dimensionized on the experimental test bed of INSA Lyon. We retake the geometry of the nozzle and generating boundary conditions. Because we cannot describe the transfer effects in the admission chamber with our model, our computational domain only begins around the middle of the converging nozzle. The computational observation domain is 0.320 m long for $0.180 < x < 0.5$ with section $\Sigma$ given by

$$\Sigma(x) \;=\; \begin{cases} 0.06 + \frac{0.075-0.06}{0.307-0.015}(x - 0.015) \text{ if } 0.180 < x < 0.307, \\ 0.0075 \text{ if } 0.307 \leq x < 0.322, \\ 0.0075 + \frac{0.045-0.075}{0.500-0.322} \text{ if } 0.322 \leq x < 0.500. \end{cases}$$

At the left entrance boundary, the flow is supersonic so that we have to impose three conditions. Deberne has communicated us the measured data at this precise location, which corresponds to a two-phase state with almost homogeneous velocity and thermodynamic

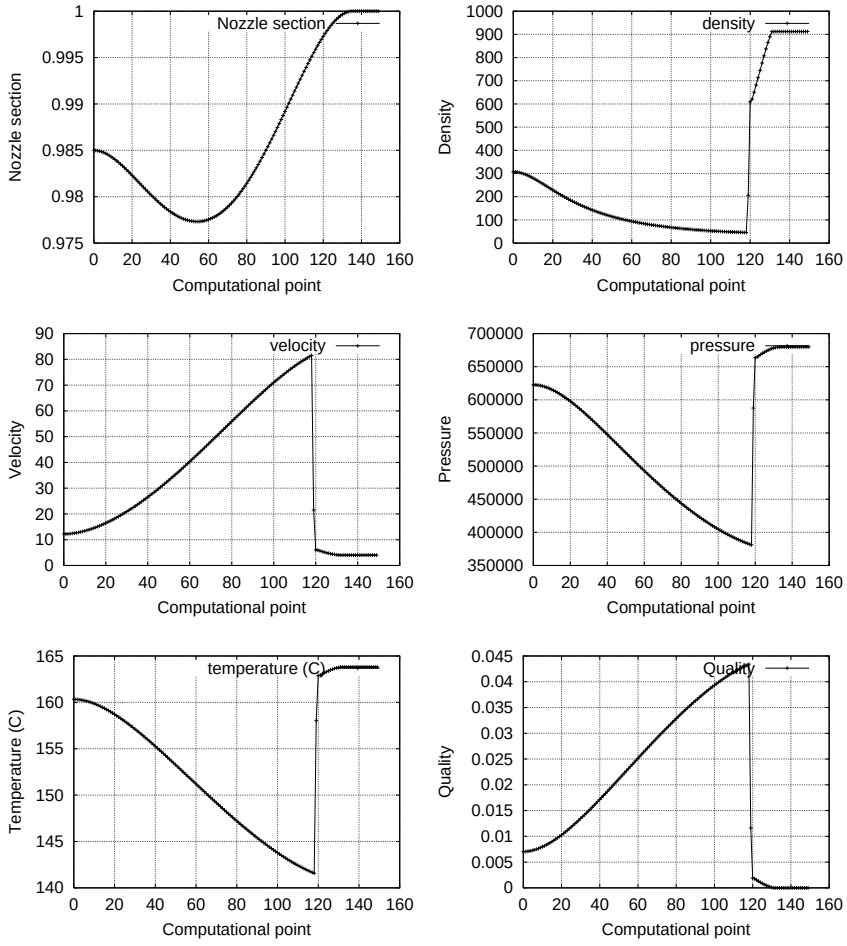


Figure 3: Profiles of steady solutions for the 6 bar injector-condenser test case

equilibrium conditions (in SI unit) :

$$\rho \;=\; 127.06228, \quad u \;=\; 6, \quad h \;=\; 355380.272.$$

Using the same strategy as described above, we have tried to identify a large range of process for this injector-condenser. We have been again confronted with the problem of robustness due to the lack of regularity of the flux at transition points which has limited our exploration of the operating range of the device. On figure 4, we present results obtained for an outlet pressure increased to about 0.25 bar.

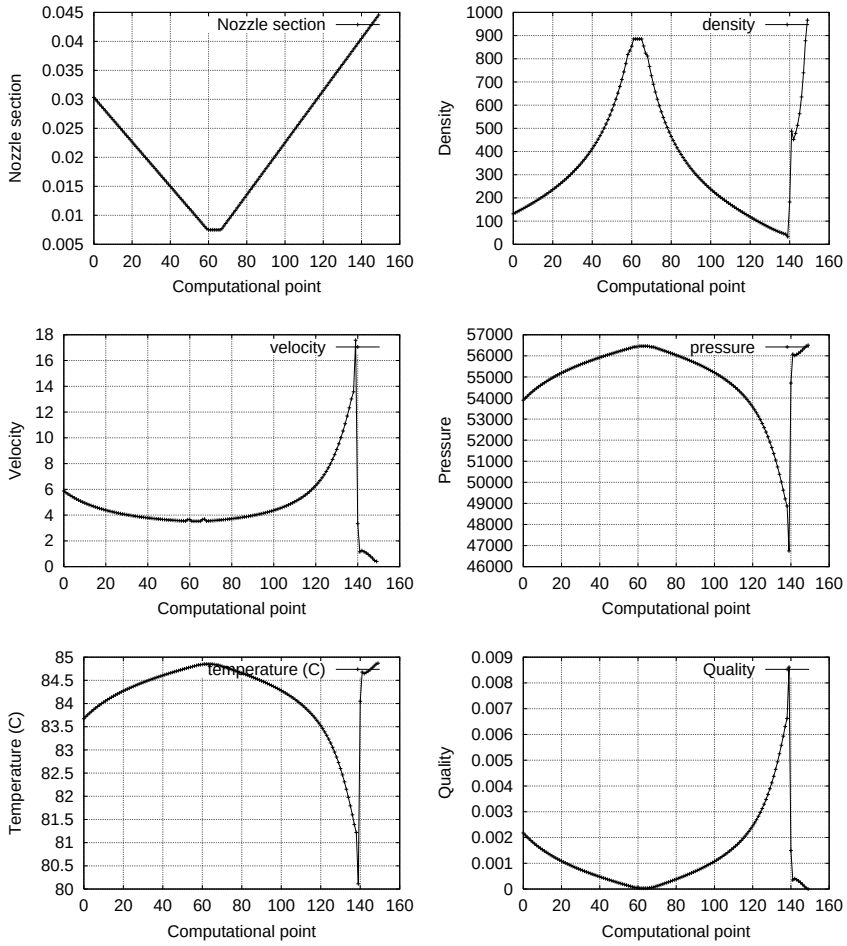


Figure 4: Profiles of steady solutions for the INSA injector-condenser device

# 7 Applications on other complex flows

## 7.1 Boiling water in a hot channel

It consists in heating some water in a channel of constant section. For that purpose, we add a source term of heat flux between the wall and the water. The vector source term is independent of the state and equal to $S(v) = {}^t(0, 0, \Phi(x,t))$ where then function $\Phi$ is described below. We suppose a slight nonequilibrium on velocity with constant relative velocity equal to $u_r = 0.1$. We decide that at the inflow, the fluid is expected to be made of pure undersaturated liquid. The heat flux $\Phi$ is calculated in such a way that the fluid at the outflow is made of dry oversaturated vapour. In that way, we should observe at the steady flow three regions of fluid of different nature separated by two points of phase transition. We do not know a priori the position of the phase transitions so that this consists in solving a free boundary problem. This academic problem let us verify the capacity of the method to correctly select the proper equations of state according to the nature of the fluid.
Channel is 7 meter long. We choose $\Sigma = 1$ and use 30 computational points with a constant space step. The flow is aimed at staying subsonic and evolving near 1 bar. Because of this last requirement, we use the constants of the model given at table 1. For the boundary conditions, we impose at the entrance the mass flux $\rho u = 1$ and the specific enthalpy which is compatible with a liquid of pressure 1 bar and temperature 50 degrees Celcius. At the outlet, we impose a pressure equal to 1 bar. The initial flow is a uniform liquid flow with values $p = 1$ bar, $T = 50$ C and $\rho u = 1$. For the heat flux function, we choose

$$\Phi(x,t) \;=\; \begin{cases} \Phi_{max}\ \min\left(\frac{t}{5000}, 1\right)\ \left(x + x^2(1-x)\right) & \text{if } 0 < x < 1 \\ 450000\ \min\left(\frac{t}{5000}, 1\right) & \text{if } 1 < x < 3.5 \\ + \text{ symmetry for } 3.5 < x < 7\,. \end{cases}$$

What has been designed in order to grow regularly according o a time variable and to fall down to zero at the boundary conditions to avoid additional difficulties linked to the treatment of the source terms at the boundary. The maximum value "450000" has been set so that the fluid is made of dry vapour at the outlet once the steady stake is reached.
The implicit method enables us to use CFL numbers up to 50000, leading to very small times of computation of order 1 minute on Sun Ultra platforms. But we acknowledge problems of robustness at the liquid - mixture phase transition during the unsteady flow even when using the flux correction discussed in section 4.2. That constrained us to strongly reduce the CFL number (down to one) during the phase of stabilization of the phase transition points. On figure 5, we present numerical results for the steady flow. They are in very good agreement with the theoretical solution which can be exhibited in one space dimension by integrating the ODEs. In particular, we have verified that, for $u_r = 0$, the quality linearly varies from zero to one in the two-phase mixture region. We verify that the pressure stays in the vicinity of 1 bar.

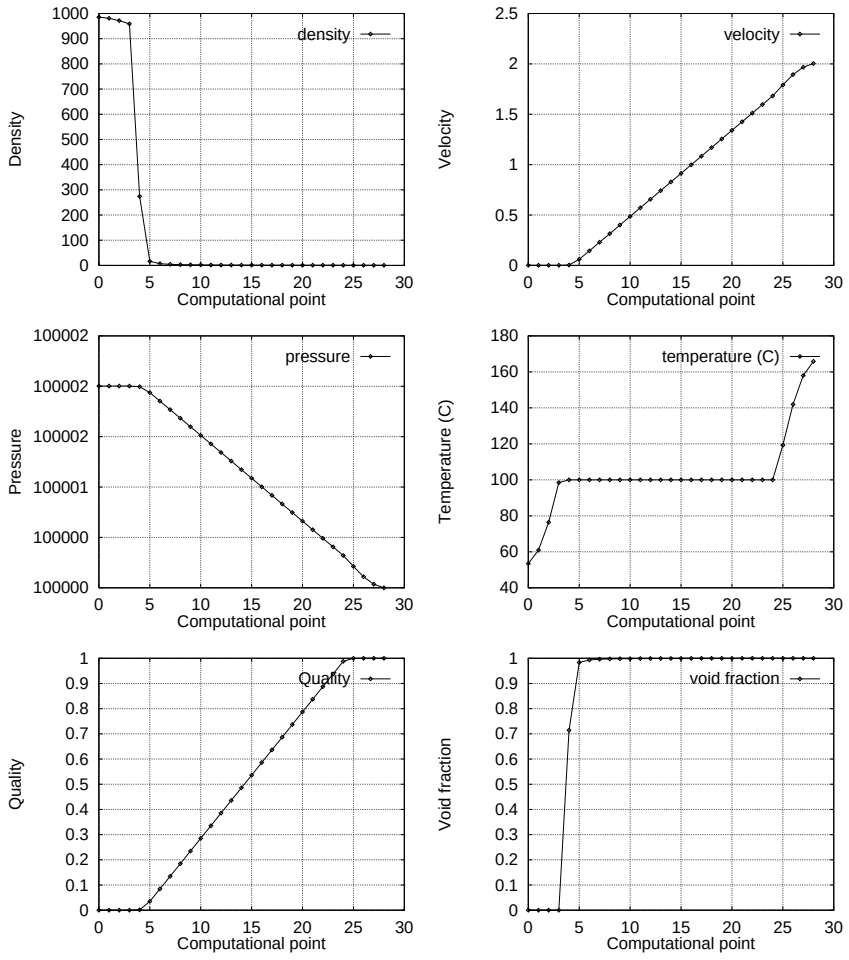


Figure 5: Profiles of steady solutions for the boiling water problem

### 7.2 Fall of pressure in a crack by friction

The problem consists in simulating the flow of water into a crack that connects two reservoirs. Such critical configurations can be encountered in tubes of vapour generators of nuclear power stations where the width of the cracks does not exceed 10 microns, but the critical mass flux can reach 5 $m^3h^{-1}$. Generally, the engineers want to known the critical mass flux for a given shape of crack and generating pressure conditions in reservoirs. The critical mass flux corresponds to a maximum mass flux and is observed when a sonic point condition is reached at the crack outlet. This is the limit case of boundary conditions where one information comes back up from the outflow expressed by the imposed pressure.
For our simulation, we suppose that the velocity field is homogeneous ($u_r = 0$) and that the section of the crack is constant, equal to $10^{-5}$ m. The friction at the crack lining induces the fall of pressure. It is modelized by a term of type

$$S_2(v) \;=\; -k\Sigma\rho u\,|u|,$$

where $k$ is a friction constant. It also induces a source term on the energy equation $S_3(v) = S_2\,u$. The *Electricité de France* subdivision department DER/RNE/TTA has realized an experimental test bed for crack flows. One has concluded that the effects of metastable saturated liquid could not be neglected to get a realistic simulation (see Pagès and Lebonhomme [40]). That is why we enrich our model here by adding two equations. The first one expresses the evolution of the fraction $X$, $0 \leq X \leq 1$ of liquid which is metastable. The source term expresses the relaxation to the saturated liquid. Written under a conservative form, this gives

$$\frac{\partial}{\partial t}\left(\rho\Sigma X\right) + \frac{\partial}{\partial x}\left(\rho u\Sigma X\right) \;=\; -\,\frac{\Sigma\rho X}{\Delta t_{rel}}, \tag{32}$$

where the characteristic time of relaxation $\Delta t_{rel}$ has to be modelized. The second equation expresses the isentropic evolution of the metastable liquid at entropy $s_{l;met}$:

$$\frac{\partial}{\partial t}\left(\rho\Sigma s_{l;met}\right) + \frac{\partial}{\partial x}\left(\rho u\Sigma s_{l;met}\right) \;=\; 0. \tag{33}$$

The new conservative system of five equations has to be closed. A metastable liquid can be associated to a metastable temperature $T_{met}$ which is a function of the entropy $s_{l;met}$ and pressure $p$. From section 4, we deduce the law

$$T_{met} \;=\; T_{met}(p, s_{l;met}) \;=\; T_0 \exp\left(\frac{s_{l;met} - s_l^0 - \eta(p - p_0)}{c_l^0}\right).$$

We also define metastable specific volume and enthalpy by

$$\tau_{l;met}(p, s_{l;met}) \;=\; \tau_l(p, T_{met}(p, s_{l;met})), \quad h_{l;met}(p, s_{l;met}) \;=\; h_l(p, T_{met}(p, s_{l;met})).$$

Specific volume and enthalpy for the mixture are then defined as

$$\begin{aligned}
\tau \;&=\; \tau(C, p, X, s_{l;met}) \;=\; C\tau_{v;sat}(p) + (1 - C - X)\tau_{l;sat}(p) + X\tau_{l;met}(p, s_{l;met}),\\
h \;&=\; h(C, p, X, s_{l;met}) \;=\; Ch_{v;sat}(p) + (1 - C - X)h_{l;sat}(p) + Xh_{l;met}(p, s_{l;met}),
\end{aligned}$$

where $\tau_{v;sat}(p) = \tau_v(p, T_{sat}(p))$ and $\tau_{l;sat}(p) = \tau_l(p, T_{sat}(p))$. In one-phase flows, we use the same model as presented for the injector-condenser.

For the simulation, we use 29 computational points. The crack length $L$ is equal to 7. Because we have encountered some difficulties with the source term of friction, we use a quite complex function of friction coefficient :

$$\begin{aligned} k(x,t) &= k_{max}\ x\ r(t) \text{ if } x < 1\,, \\ &= k_{max}\ r(t) \text{ if } 1 \leq x < 5\,, \\ &= k_{max}\,(1-(x-5)))\ r(t) \text{ if } 5 \leq x < 6\,, \\ &= 0 \text{ if } 6 \leq x \leq 7\,, \end{aligned}$$

where $k_{max} = 3\,500\,000$ and $r(t) = \min\left(1, \frac{t}{2.5}\right)$. We still have to model the characteristic time $\Delta t_{t;rel}$. For our preoccupations of qualification and validation of the method, we only use a term that ensures the fall of $X$ to zero at the end of the computational domain, namely

$$\Delta t_{rel}(x) \ = \ \frac{1}{2}\ \max\left(\frac{L-x}{\sqrt{u^2+\epsilon^2}}, \frac{\Delta x}{\sqrt{u^2+\epsilon^2}}\right),$$

where $\epsilon$ is a small parameter, here chosen equal to $10^{-2}$. For a more realisatic relaxation model see the discussion in [40]. At the entrance, we impose $\rho u = 10$ and $h$ compatible with a pure liquid at temperature $T = 99.5$ C. When the first vapour bubbles appear, we suppose that the liquid phase is almost completely metastable, with $X = 0.999$ and metastable temperature $T_m = T$. Outlet boundary conditions are $p = 50\,000$ Pa. The initial flow is liquid, uniform with data $\rho u = 10$, $p = 1$ bar, $X = 0.999$ and $T_m = T = 99.5$ C. On figure 6 the numerical solutions are presented after convergence to the steady flow. The thermodynamic quantities evolve correctly. Boiling conditions are reached; the quality increases up to $C = 0.0318$ at the outlet. One can observe the brutal acceleration of the fluid at the end of the computational domain due to the quadratic nature of the friction source term. The problem is difficult to solve because of large characteristic time ratios between convection and return to local equilibrium. Thus, CFL numbers could not exceed the value of 5 during the computation. At the outlet boundary condition, the sonic point conditions are not reached yet because of difficulties encountered with this problem. The slope on pressure profile should tend to $-\infty$ at sonic conditions, which is not reached here but the numerical profile is not so far from a such singular behaviour. We are still working on the critical mass flux and the treatment of sonic boundary conditions.

# 8 Conclusion and future work

By this paper, we have shown the capacity of the Characteristic Flux Method to capture two-phase flows. The example of the HEM model is not restrictive and the method could be extended to finer models like those with six equations. We set a general numerical test bed with a very adaptive and modular code written in C++. A large part of this code is independent of the model and equations which can enable to compare models at fixed

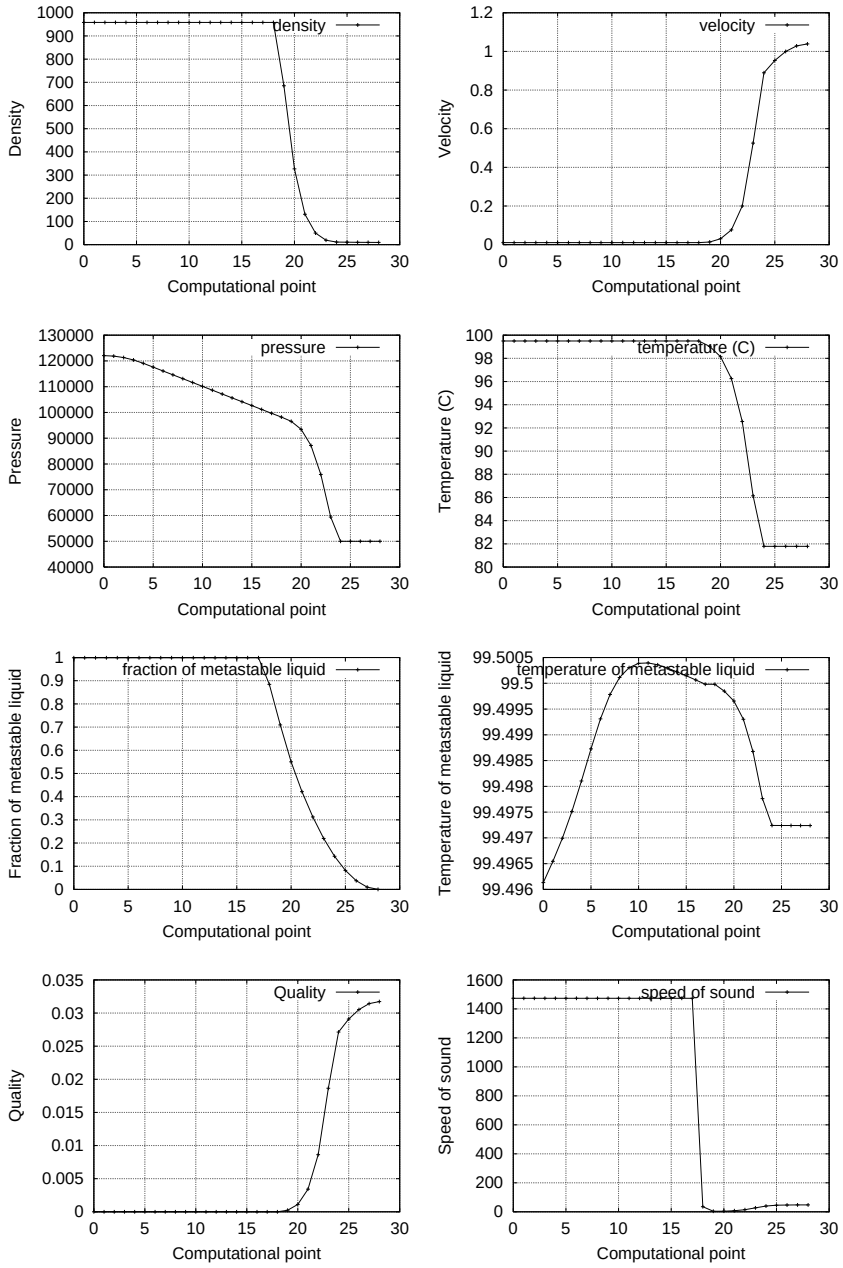


Figure 6: Profiles of steady solutions for the problem of fall in pressure using ECREVISSE model

problem. We have also presented a way to set very simple equations of state that accelerate the computation. Of course, it is as accurate as when using spline-based tabulated laws, but this is sufficient for us to heighten difficulties inherent to two-phase flows. Anyway, this is first of all a trick to get faster computations, but of course water tables can be used. The simulations on complex one-dimensional flows have then shown the capacity of the method to deal with regions of strong gradient of density or with free boundary phase transition. But it reveals a lack of robustness at phase transitions which has not been completely understood yet. It would seem that the fully implicit method is multivaluated and this feature is more sensible when discontinuities on Jacobian matrices are present.
The current research is aimed at achieving a variant of the Flux Scheme method that is entropy satisfying and that intrinsically takes into account the phase transition feature in its script.

**Acknowledgments**

The present work was done in the framework of a collaboration between *Electricité de France DR&D, Département Mécanique des Fluides et Transferts Thermiques* and the *Centre de Mathématiques et de Leurs Applications, ENS Cachan-CNRS*, France.

# 9 Appendix A : Derivation of the Homogeneous Equilibrium Model

In this Appendix, our aim is to describe how the Homogeneous Equilibrium Model can be derived from a 6 equation two-fluid model. In the setting of the so-called averaged model (see *e.g.* ISHII [34]), the description of the flow of a diphasic mixture is given in terms of phasic variables. In the case of a quasi-1D flow, the evolution equations describing the balances of mass, momentum and total energy read as follows :

$$\frac{\partial \alpha_v \rho_v \Sigma(x)}{\partial t} + \frac{\partial \alpha_v \rho_v u_v \Sigma(x)}{\partial x} = \Sigma(x)\Gamma_{l\to v}\,, \tag{34}$$

$$\frac{\partial \alpha_\ell \rho_\ell \Sigma(x)}{\partial t} + \frac{\partial \alpha_\ell \rho_\ell u_\ell \Sigma(x)}{\partial x} = \Sigma(x)\Gamma_{v\to l}\,, \tag{35}$$

$$\frac{\partial \alpha_v \rho_v u_v \Sigma(x)}{\partial t} + \frac{\partial (\rho_v u_v^2 + p)\alpha_v \Sigma(x)}{\partial x} = p\frac{\partial \alpha_v \Sigma(x)}{\partial x} + \Sigma(x)(f_{l\to v} + \Gamma_{l\to v} u_{l,v})\,, \tag{36}$$

$$\frac{\partial \alpha_\ell \rho_\ell u_\ell \Sigma(x)}{\partial t} + \frac{\partial (\rho_\ell u_\ell^2 + p)\alpha_\ell \Sigma(x)}{\partial x} = p\frac{\partial \alpha_\ell \Sigma(x)}{\partial x} + \Sigma(x)(f_{v\to l} + \Gamma_{v\to l} u_{v,l})\,, \tag{37}$$

$$\begin{aligned}\frac{\partial \alpha_v \rho_v (e_v + u_v^2/2)\Sigma(x)}{\partial t} + \frac{\partial \rho_v u_v (e_v + p/\rho_v + u_v^2/2)\alpha_v \Sigma(x)}{\partial x} = \\ = -p\frac{\partial \alpha_v \Sigma(x)}{\partial t} + \Sigma(x) Q_{l\to v}\,,\end{aligned} \tag{38}$$

$$\begin{aligned}\frac{\partial \alpha_\ell \rho_\ell (e_\ell + u_\ell^2/2)\Sigma(x)}{\partial t} + \frac{\partial \rho_\ell u_\ell (e_\ell + p/\rho_\ell + u_\ell^2/2)\alpha_\ell \Sigma(x)}{\partial x} = \\ = -p\frac{\partial \alpha_\ell \Sigma(x)}{\partial t} + \Sigma(x) Q_{v\to l}\,.\end{aligned} \tag{39}$$

Let us now describe the physical meaning of each variables : $\alpha_i$ is the volume fraction of the fluid $i$, $\rho_i$ is the density of the fluid $i$, $u_i$ denotes the velocity of the phase $i$ and $p$ is the thermodynamic pressure. Denoting by $e_i$ the specific internal energy of the phase $i$, we have set $E_i = e_i + \frac{1}{2}|u|^2$ : the total specific energy of the fluid $i$ and $H_i = E_i + \frac{p}{\rho_i}$ the total specific enthalpy of the fluid $i$ (we shall also use the notation $h_i \equiv e_i + \frac{p}{\rho_i}$ for the specific enthalpy of the fluid $i$).

We have the relation $\alpha_v + \alpha_\ell = 1$ and in order to close the system (34) to (39), we have to write two equations of state :

$$F_i(p, \rho_i, e_i) = 0\,, i = 1, 2\,. \tag{40}$$

The right hand sides of equations (34), (35) contain mass transfer terms $\Gamma_{v\to\ell}$ and $\Gamma_{\ell\to v}$ which satisfies $\Gamma_{v\to\ell} + \Gamma_{\ell\to v} = 0$. Similarly, equations (36), (37) contain momentum transfer

terms $f_{\ell\to v} + \Gamma_{\ell\to v} u_{\ell,v}$ and $f_{v\to\ell} + \Gamma_{\ell\to v} u_{\ell,v}$ with $f_{\ell\to v} + f_{v\to\ell} = 0$. Finally, equations (38), (39) contain momentum transfer terms $Q_{v\to\ell}$ et $Q_{\ell\to v}$ with $Q_{v\to\ell} + Q_{\ell\to v} = 0$.
Introducing the mean variables : $\rho = \alpha_v\rho_v + \alpha_\ell\rho_\ell$ , $\rho u = \alpha_v\rho_v u_v + \alpha_\ell\rho_\ell u_\ell$ , $\rho E = \alpha_v\rho_v E_v + \alpha_\ell\rho_\ell E_\ell$ , and the quality $C \equiv \alpha_v\rho_v/\rho$ together with the relative velocity $u_r \equiv u_v - u_\ell$, we obtain equations (1) to (3) by simply adding two by two the phasic equations, once the total energy is defined by (4) and the latent heat by $L \equiv h_v - h_\ell$.

# 10 Appendix B : The approximate problem from Homogeneous Equilibrium model

we should stress on whether the system (1) to (3) is its hyperbolic or not. Since this property is independent of $\Sigma$, we take $\Sigma \equiv 1$). This question is more simply investigated with the following quasilinear formulation :

$$\rho_t + (\rho u)_x = 0, \tag{41}$$

$$u_t + uu_x + \frac{1}{\rho}(p + C(1-C)u_r^2)_x = 0\,, \tag{42}$$

$$s_t + us_x + \frac{1}{\rho}(\rho C(1-C)\frac{L}{T}u_r)_x = 0\,, \tag{43}$$

where the specific entropy function $s$ is defined thanks to the two first laws of thermodynamics ($\tau \equiv 1/\rho$) :

$$Tds = de + pd\tau\,. \tag{44}$$

**Proposition 7** *We assume that the slip velocity $u_r$ is a given constant. Denoting by $\Pi$ and $\Phi$ the two functions of the 2 independent variables $\rho$ and $s$, $\Pi \equiv p + C(1-C)u_r^2$ and $\Psi \equiv \rho C(1-C)\frac{L}{T}u_r$, the system (41) to (43) will have real characteristics if and only if*

$$\begin{aligned}\Delta \equiv 36\left(\frac{\partial\Pi}{\partial\rho}\right)^3\rho^4 - 72\left(\frac{\partial\Pi}{\partial\rho}\right)^2\rho^2\left(\frac{\partial\Psi}{\partial s}\right)^2 + 36\left(\frac{\partial\Pi}{\partial\rho}\right)\left(\frac{\partial\Psi}{\partial s}\right)^4 + \\ 324\left(\frac{\partial\Psi}{\partial s}\right)\left(\frac{\partial\Pi}{\partial\rho}\right)\rho^2\left(\frac{\partial\Psi}{\partial\rho}\right)\frac{\partial\Pi}{\partial s} - 36\left(\frac{\partial\Psi}{\partial s}\right)^3\left(\frac{\partial\Psi}{\partial\rho}\right)\frac{\partial\Pi}{\partial s} - \\ 243\,\rho^2\left(\frac{\partial\Psi}{\partial\rho}\right)^2\left(\frac{\partial\Pi}{\partial s}\right)^2 \geq 0\,.\end{aligned} \tag{45}$$

*Moreover when $\Delta > 0$, the three roots are distinct.*

*Proof.* We linearize system (41) to (43) around a constant state $(\rho, u, s)$ and look for nonvanishing plane wave solutions $Ve^{i(kx-\omega t)}$. Real characteristics will correspond to the case where the only possible solutions occur for $k$ and $\omega$ real. This amounts to saying that the roots of the characteristic polynomial are real. This polynomial is here

$$\lambda^3 + \frac{1}{\rho}\frac{\partial\Psi}{\partial s}\lambda^2 - \frac{\partial\Pi}{\partial\rho}\lambda + \frac{1}{\rho}\left(\frac{\partial\Psi}{\partial\rho}\frac{\partial\Pi}{\partial s} - \frac{\partial\Pi}{\partial\rho}\frac{\partial\Psi}{\partial s}\right)\,, \tag{46}$$

and the result follows by simply computing its discriminant.

**Remark 1** *In the case where $u_r \equiv 0$, as expected, condition (45) reads as* $\left(\frac{\partial p}{\partial \rho}\right)_s \geq 0\,.$

# 11 Appendix C : equation of state, respect of the first principle of Thermodynamics and entropies

Let first consider the one-phase fluid case (pure liquid or dry vapour). The first principle of Thermodynamics stipulates that

$$\frac{1}{T}\, de \;+\; \frac{p}{T}\, d\tau$$

is the total differential of a function, see (44). Since $h = e + p\tau$, we can also write

$$ds = \frac{1}{T}\, dh - \frac{\tau}{T}\, dp. \tag{47}$$

The compatibility relation on the crossed partial derivatives leads to the two first constraints

$$\left(\frac{\partial h}{\partial p}\right)_T \;=\; -T^2 \left(\frac{\partial}{\partial T}\left(\frac{\tau}{T}\right)\right)_p \tag{48}$$

for both the liquid and the vapour phases. Once expression (48) holds true, the expression of the entropy $s_k$ of each phase ($k = v$ or $l$) is then deduced from (47) by integrating.

Let us consider now the mixture case. To express the first principle of Thermodynamics in that case, it is convenient to introduce the latent heat $L$ defined as the difference of enthalpies between the two phases in the saturated mixture

$$L(T) = h_{v;s}(T) - h_{l;s}(T). \tag{49}$$

If we express the differential function of the enthalpy function of $L$ and $C$

$$dh = \left(C\,\frac{dL}{dp} + \frac{dh_\ell}{dp}\right) dp + L\, dC, \tag{50}$$

and inject it in (47), this shows that

$$\frac{L}{T}\, dC + \frac{c\frac{dL}{dp} - \tau + \frac{dh_\ell}{dp}}{T}\, dp$$

is a total differential. It is true if and only if

$$\frac{\partial}{\partial p}\left(\frac{L}{T}\right) = \frac{\partial}{\partial C}\left(\frac{C\frac{dL}{dp} + \frac{dh_\ell}{dp} - \tau}{T}\right)\,. \tag{51}$$

This third constraint is written quite simply as

$$L\frac{dT}{dp} = T(\tau_v - \tau_\ell)\,. \tag{52}$$

This is the famous Clapeyron's law. The entropy law of the mixture can be deduced by integrating (52) :

$$s = \frac{C\,L}{T} - \int_{p_0}^{p} \frac{\tau_\ell - \frac{dh_\ell}{dp}}{T} dp\,. \tag{53}$$

Let us now denote by $c_v$ the mass heat of saturated vapour and by $c_\ell$ the heat mass of saturated liquid. We then have by definition of the $c_k$'s

$$T ds_k = c_k\, dT \text{ for } k \in \{v, l\}\,. \tag{54}$$

This can be rewritten, using (47), as

$$c_k = \left( \frac{dh_k}{dT} - \tau_k \frac{dp_s}{dT} \right)\,. \tag{55}$$

Thus, coupling with Clapeyron's law (52), we have

$$c_v - c_\ell = \frac{dL}{dT} - \frac{L}{T}\,, \tag{56}$$

and

$$\tau_\ell - \frac{dh_\ell}{dp} = -c_\ell \frac{dT}{dp}\,, \tag{57}$$

$$s \;=\; \frac{c\,L}{T} + \int_{T_0}^{T} \frac{c_\ell}{T} dT\,. \tag{58}$$

In our context of water flow, it is reasonable to suppose that when $c_\ell$ is constant, then 58 becomes

$$s \;=\; \frac{cL}{T} + c_\ell^0 \log \frac{T}{T_0}\,. \tag{59}$$

**First reduction**

**Lemma 1** *Suppose that the law $\tau_v(p,T)$ is of the form*

$$\tau_v(p,T) \;=\; T\ \kappa(p) \tag{60}$$

*for a given function $\kappa$. In addition to this, let's suppose more that $\tau_\ell$ has the form*

$$\tau_\ell(p,T) \;=\; \varphi_1(p) \;+\; \varphi_2(T). \tag{61}$$

*and that the function*

$$h_\ell(p_0,T) \;=\; \varphi(T) \tag{62}$$

*is a known function at a given pressure $p_0$. Then the specific enthalpy of the vapour $h_v$ is a function $\Psi$ of the only temperature and $h_\ell$ and $\Psi$ are given by*

$$h_\ell(p,T) \;=\; \varphi(T) + \int_{p_0}^{p} \varphi_1(q)dq + \left(\varphi_2(T) - T\varphi_2'(T)\right)(p - p_0) \tag{63}$$

$$\begin{aligned} \Psi(T) \;=\; & \varphi(T) + \int_{p_0}^{p_s(T)} \varphi_1(q)dq - T^2 \left(\varphi_2(T)/T\right)'(T)\,(p_s(T) - p_0) \\ & + T p_s'(T)\ \left(T\kappa(p_s(T)) - \varphi_1(p_s(T) - \varphi_2(T)\right). \end{aligned} \tag{64}$$

*The liquid, vapour and mixture entropies are given by*

$$s_\ell(p,T) = s_\ell^0 + \int_{T_0}^{T} \frac{\varphi'(t)}{t} dt - \varphi_2'(T)(p-p_0) - [\varphi_2'(T) - \varphi_2'(T_0)](p-p_0), \quad (65)$$

$$s_v(p,T) = s_v^0 + \int_{T_0}^{T} \frac{\Psi'(t)}{t} dt - [\lambda(p) - \lambda(p_0)], \quad (66)$$

$$s(C,T) = Cs_{v;s}(T) + (1-C)s_{l;s}(T) \quad (67)$$

$$= s_0 + \frac{CL}{T} + \int_{T_c}^{T} \left[ \frac{\varphi'(t)}{t} - \varphi_2''(t)(p_s(t) - p_c) - \varphi_2'(t)p_s'(t) \right] dt.$$

*Proof.* The fact that $\tau_v = \Psi(T)$ is an immediate consequence of (48) under (60). Expression (63) is obtained on an integration of 48 for the liquid phase using (62). Expression (64) is only Clapeyron's law (52) under the hypotheses of the lemma.

We see that we have five real unknown functions $p_s(T)$, $\kappa$, $\varphi(T)$, $\varphi_1(p)$ and $\varphi_2(T)$. If the primitive of $\varphi_1$ is known, then the laws on $h_\ell$ and $h_v$ become explicit using expressions (63) and (64).

**Second reduction : choice for the pressure of saturation**

**Lemma 2** *Let us keep the hypotheses of lemma 1 and denote by $\lambda$ a primitive function of $\kappa$. If $p_s(T)$ is the solution of the differential equation*

$$\frac{d}{dT}\left[\lambda(p_s(T))\right] = \frac{L_0}{T^2} \quad (68)$$

*for a given constant $L_0$, then*

$$\Psi(T) = h_{l;s}(T) + L_0 \left(1 - \frac{\tau_{l;s}(T)}{\tau_{v;s(T)}}\right). \quad (69)$$

**Remark 2** *Lemma 2 shows that, under the additional hypothesis (68) and because $\tau_{l;s} << \tau_{v;s}$ in the case of water, the specific vapour enthalpy is almost a constant $L_0$. This approximation is reasonable for the water. So it is also normal to calibrate $L_0$ as the latent heat for given conditions of saturation. The remaining unknown functions are then $\varphi$, $\varphi_1$, $\varphi_2$ and $\kappa$.*

**Remark 3** *The differential equation (68) is just Clapeyron's law, altered with the following approximations : the latent heat is approximated by a constant $L_0$, $\tau_{v;s} - \tau_{l;s}$ is approximated by $\tau_{v;s}$, and $\tau_v$ has the form (60). Under these assumptions, we have*

$$L_0 \frac{dT_s}{dp} = T\tau_{v;s} = T^2\kappa(p_s)$$

*so that*

$$\frac{L_0}{T^2} = p_s'(T)\kappa(p) = \frac{d\lambda(p_s(T))}{dT}.$$

### 11.0.1 Examples of partly linear or parabolic laws of state

To close the formulae, we decide to use either a linear or a quadratic function for $\varphi_1$, $\varphi_2$ or $\varphi$ and a "simple" function $\kappa$.

**Proposition 8** *Let us choose*

$$\kappa(p) = \frac{R}{p}, \tag{70}$$

$$\tau_\ell(p,T) = \tau_\ell^0 + \xi(p-p_0) + \eta\,(T-T_0) + \frac{\nu}{2}(T-T_0)^2\,, \tag{71}$$

$$\varphi(T) = h_\ell^0 + c_\ell^0(T-T_0). \tag{72}$$

$$\tag{73}$$

*Then, it comes*

$$p_s(T) = p_c\ \exp\left[\frac{L_0}{R}\left(\frac{1}{T_c}-\frac{1}{T}\right)\right]. \tag{74}$$

$$\begin{aligned} h_\ell(p,T) &= h_\ell^0 + c_\ell^0(T-T_0) - \nu(T^2-T_0^2)p + (\tau_\ell^0 - \eta T_0)(p-p_0) \\ &\quad + \frac{\xi}{2}(p-p_0)^2\,, \end{aligned} \tag{75}$$

$$h_v(T) = \psi(T) = h_\ell(p_s(T),T) + L_0\left(1 - \frac{\tau_{ls}(T)}{\tau_{vs}(T)}\right), \tag{76}$$

$$\tag{77}$$

*with entropies*

$$\begin{aligned} s_\ell(p,T) &= s_\ell^0 - [\eta + 2\nu(T-T_0)](p-p_0) + c_\ell^0 \log\frac{T}{T_0}\,, \\ s_v(p,T) &= s_v^0 - R\log\frac{p}{p_0} + \int_{T_0}^{T}\frac{\psi'(t)}{t}dt\,, \\ s(C,T) &= s_0 + \frac{C\,L}{T} - [\eta + \nu(T-T_0)](p_s(T)-p_c) + c_\ell^0\log\frac{T}{T_c}\,. \end{aligned}$$

### 11.0.2 Computation of constants of the model using water tables

We now have to end up with the equations of state by providing physical values for all these constants. This is reached by using the tables of water. We first choose a range of variation for the pressure and temperature. Then we choose constant states $(\tau(p_0,T_0), h(p_0,T_0))$ and deduce from the table derivates quantities such as $\frac{\partial\tau}{\partial p}_{|T=T_0}$ or $\frac{\partial\tau}{\partial T}_{|p=p_0}$. The values presented on tables 1 and 2 are obtained for a pressure respectively close to 1 bar and 6 bar, and for a temperature close to the saturation conditions. Finally, on figure 7 we compare these analytical equations of state with constants of Table 1, to real data extracted from VDI water tables. We do observe that our laws thoroughly match the VDI tables for a pressure

| | | | |
|---|---|---|---|
| $\xi$ | $-5.36e-13$ | $L_0$ | $2300e3$ |
| $\eta$ | $6.22e-7$ | $R$ | $456.31$ |
| $p_0$ | $1.1e5$ | $\tau_\ell^0$ | $1.0438e-3$ |
| $T_0$ | $373.15$ | $h_\ell^0$ | $418.9e3$ |
| $p_c$ | $1.013e5$ | $c_\ell^0$ | $4194.$ |
| $T_c$ | $373.15$ | | |

Table 1: Table of constants used for a range of pressure or order 1 bar

| | | | |
|---|---|---|---|
| $\xi$ | $-6.40e-13$ | $L_0$ | $2085.08e3$ |
| $\eta$ | $7.843e-7$ | $R$ | $443.032$ |
| $p_0$ | $6.0e5$ | $\tau_\ell^0$ | $1.0698e-3$ |
| $T_0$ | $403.15$ | $h_\ell^0$ | $546.525e3$ |
| $p_c$ | $6.e5$ | $c_\ell^0$ | $4200.$ |
| $T_c$ | $432.0$ | | |

Table 2: Table of constants used for a range of pressure or order 6 bar

in a range from 0.5 bar to 6 bar and for a temperature near saturation conditions. Errors on vapor specific enthalpy profiles are more noticeable because of the lack of freedom on these laws due to the constraint for respecting the entropy. One can notice a relative error of about 3 percent on enthalpy near 1 bar. But this is sufficient to validate numerical methods, or to compute intermediate results before applying more accurate tabulated laws for example.

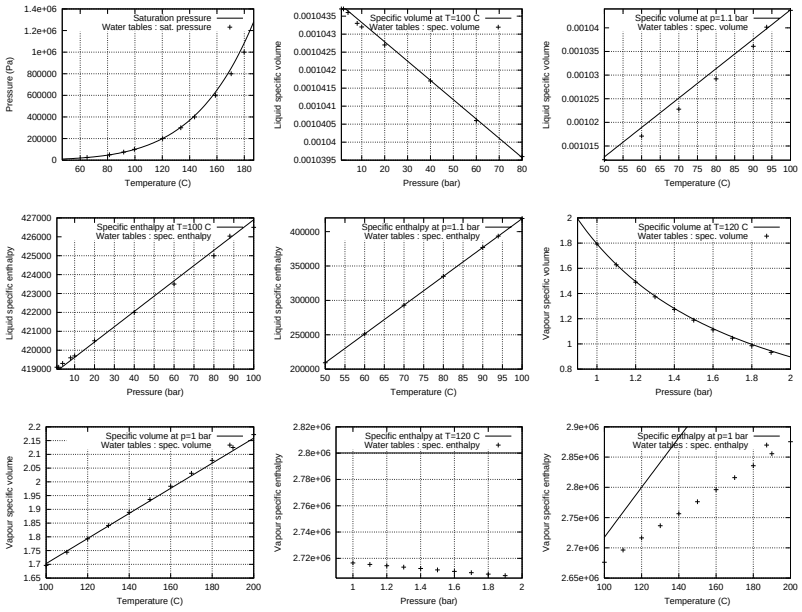


Figure 7: Comparison between analytical equations of state and water tables: saturation pressure, liquid and vapor specific volume and enthalpy. Model constants available in a vicinity of $p = 1$ bar and saturation

# References


[1] ALOUGES F., GHIDAGLIA J.-M. and TAJCHMAN M., On the interaction of upwinding and forcing for nonlinear hyperbolic systems of conservation laws, Prépublication du CMLA and article to appear, 1999.

[2] BESTION D., The physical closure laws in the CATHARE code, Nucl. Eng. Design, 124, 229-245, 1990.

[3] BOURE J.A. and DELHAYE J.-M., General Equations and Two-Phase Flow Modeling, in *Handbook of Multiphase Systems*, G. Hestroni, Ed., Hemisphere, 1982.

[4] BOUCKER M., *Modélisation numérique multidimensionnelle d'écoulements diphasiques liquide-gaz en régimes transitoires et permanents : méthodes et applications*, Thèse, ENS-Cachan, France, 1998.

[5] BOUCHUT F., Entropy satisfying flux vector splittings and kinetic BGK models, to appear in Num. Math., 2002.

[6] BOUCKER M. and GHIDAGLIA J.-M., On the discretization of non conservative terms in the context of multidimensional flux schemes, in preparation.

[7] COCCHI J.P. and SAUREL R., A Riemann Problem Based Method for Compressible Multifluid Flows, J. Comput. Phys., 137, 265-298, 1987.

[8] COQUEL F., EL AMINE K., GODLEWSKI E., PERTHAME B. and RASCLE P., A Numerical Method Using Upwind Schemes for the Resolution of Two-Phase Flows, J. Comput. Phys., 136, 272-288, 1997.

[9] COQUEL F. and LIOU M.S., *Hybrid upwind splitting (HUS) by a field-by-field decomposition*, NASA TM-106843, Icomp-95-2 (1995).

[10] CORTES J. and GHIDAGLIA J.-M., On the dependence of the linearizing state for flux scheme, in preparation.

[11] DEBERNE N., Modélisation et expérimentation des Injecteurs-condenseurs, PhD Thesis, INSA Lyon France (2000).

[12] DECLERCQ E. , FORESTIER A., HERARD J. M., LOUIS X and POISSANT G., "An exact Riemann solver for a multicomponent turbulent compressible flow". Int. J. of Comp. Fluid Dynamics, vol.14, pp. 117-131 (2001).

[13] DE VUYST F., Construction de schémas de flux s'appuyant sur une formulation cinétique champ par champ, C. R. Acad. Sci. Série I, vol. 330(4), pp. 321-326 (2000)

[14] DE VUYST F. *et al*, Numerical modeling of two-phase water flows using flux schemes. application to the injector-condenser and boiling water in a hot channel, groupe de travail sur les schémas de flux, IESC Cargèse, 22-24 septembre 1999, electronic editions *http://www.cmla.ens-cachan.fr/Utilisateurs/perfortmans/*

[15] DE VUYST F., GHIDAGLIA J.-M. and LE COQ G., Partly linearized laws of state for modeling two-phase flows and numerical computation using flux schemes, AMIF-ESF Worshop "Computing methods for two-phase flow", Aussois, France, Jannuary 2000 and article in preparation.

[16] DE VUYST F., GHIDAGLIA J.M., LE COQ G., Mimouni S., Pagès D., partly linearized laws of state for modeling two-phase flow and numerical computation using flux schemes, Séminaire DRN/MFN, CEA Saclay, France, 24-26 janvier 2000.

[17] DREW D.A. and LAHEY R.T., Application of General Constitutive Principles to the Derivation of Multidimensional Two-Phase Flow Equations, Int. J. Multiphase Flow, 5, 243-264, 1979.

[18] DREW D.A. and WALLIS G.B., Fundamentals of Two-Phase Flow Modeling, in *Multiphase Science and Technology, Volume 8*, Hewitt *al* Editors, Begell House, Inc., New-York, 1994.

[19] FAILLE I. and HEINTZ E., A Rough Finite Volume Scheme for Modeling Two-Phase Flow in a Pipeline, Computers & Fluids, 28, No. 2, p. 213-241, 1999.

[20] GHIDAGLIA J.-M., *Une approche volumes finis pour la résolution des systèmes hyperboliques de lois de conservation*,Note, Département Transferts Thermiques et Aérodynamique, Direction des Etudes et Recherches, Electricité de France, HT-30/95/015/A, 1995.

[21] GHIDAGLIA J.-M., *On the numerical treatment of boundary conditions in the context of flux schemes*, In preparation.

[22] GHIDAGLIA J.-M., Flux schemes for solving nonlinear systems of conservation laws, *Proceedings of the meeting in honor of P.L. Roe*, Chattot J.J. and Hafez M. Eds, Arcachon, July 1998, to appear.

[23] GHIDAGLIA J.-M., KUMBARO A. and LE COQ G., Une méthode volumes-finis à flux caractéristiques pour la résolution numérique des systèmes hyperboliques de lois de conservation, *C.R.Acad. Sc. Paris*, 1996, **322**, I, 981-988.

[24] GHIDAGLIA J.-M., KUMBARO A. and LE COQ G., On the numerical solution to two fluid models *via* a cell centered finite volume method, Preprint, 2000.

[25] GHIDAGLIA J.-M., KUMBARO A., LE COQ and TAJCHMAN M., A finite volume implicit method based on characteristic flux for solving hyperbolic systems of conservation laws, *Proceedings of the Conference on : Nonlinear evolution equations and infinite-dimensional dynamical systems* (Shanga, June 1995), Li Ta-Tsien Ed., 1997, World Scientific, Singapore.

[26] GHIDAGLIA J.-M., LE COQ G. and TOUMI I., Two flux schemes for computing two phases flows throught multidimensional finite volume methods, Proceedings of the NURETH-9 conference, October 1999, San Francisco, American Nuclear Society.

[27] GHIDAGLIA J.-M. and PASCAL F., *Passerelles volumes finis - éléments finis, méthodes et applications*, Rapport EDF/DER/TTA/HT-33/99/002/A, Chatou, France, 1999.

[28] GHIDAGLIA J.-M. and PASCAL F., Passerelles volumes finis - éléments finis, C.R.Acad. Sc. Paris, I, 328, 711-716, 1999.

[29] GZ M.F. and MUNZ C.-D., Approximate Riemann Solvers for Fluid Flow with Material Interfaces, in *Numerical Methods for Wave Propagation*, E.F. Toro and J.F. Clarke, Eds., 211-235, Kluwer Academic Publishers, 1998.

[30] GUILLARD H., Mixed element volume methods in computational fluid Dunamics, *Lecture Series, Von Karman Institute for fluid Dynamics*, 1995.

[31] HALAOUA K., *Quelques solveurs pour les opérateurs de convection et leurs applications la mécanique des fluides diphasiques*, Thèse, ENS-Cachan, France, 1998.

[32] HARTEN A., LAX P.D. and VAN LEER B., *On upstream differencing and Godunov-type schemes for hyperbolic conservation laws*, SIAM Review, 25 (1983), pp. 35-61.

[33] HEWITT G.F., DELHAYE and ZUBER M., *Numerical benchmark tests, in* Multiphase Science and Technology, vol. 3, Hemisphere, Washington DC/ New York, 1987.

[34] ISHII M., *Thermo-Fluid Dynamic Theory of Two-Phase Flow*, Eyrolles, Paris, 1975.

[35] KRöNER D., *Numerical schemes for conservation laws*, Wiley Teubner, 1997.

[36] LIOU M.S., Low Mach Number and Two-Phase Flow Extensions of the AUSM Scheme, 30th VKI Computational Fluid Dynamics Lecture Series, 8-12 March, 1999.

[37] METRAL, J., Modélisation de lécoulement de plasmas dair hors-équilibre, Ecole Centrale de paris, Thesis, 2002.

[38] MIMOUNI S., BOUCKER M., LE COQ G. and GHIDAGLIA J.-M., *An overview of the VFFC-methods and tools for the simulation of two-phase flows*, Rapport EDF/DER/TTA/HT-33/99/006/A, Chatou, France, 1999.

[39] OSHER S. and SOLOMON F., "Upwind Difference Scheme for Hyperbolic Systems of Conservation Laws", Math. Comput., 38, 339-374, 1982.

[40] PAGES D. and LEBONHOMME S., Pagès D., Le Bonhomme S., *Logiciel ECREVISSE version 2.1, note de principe et notice utilisateur*, Note EDF HT-32/98/017/A, Châtou, 1998.

[41] RAMOS D., Existence and uniqueness for a mixed hyperbolic-parabolic problem, Proceedings of the workshop *Schémas de flux pour la simulation numérique des écoulements diphasiques*, Cargèse, France September 1999, http://www.cmla.ens-cachan.fr/Utilisateurs/perfortmans/ and PhD Thesis in preparation.

[42] RANSOM V.H., *Numerical Modeling of Two-Phase Flows*, Cours de l'Ecole d'été d'Analyse Numérique - CEA-INRIA-EDF, 12-23 juin 1989.

[43] RANSOM V.H. and HICKS D.L., Hyperbolic two-pressure models for two-phase flow revisited, J. Comput. Phys., 75, pp 498-504, 1988.

[44] ROE P.L., Approximate Riemann solvers, parameter vectors and difference schemes, J. Comput. Phys., 43, pp 357-372, 1981.

[45] ROMATE J.E., "Approximate Riemann Solvers for a Hyperbolic Two-Phase Flow Model", in Numerical Modelling in Continuum Mechanics, M. Feistauer, R. Rannacher and K. Kozel (Eds.), Proc. 3rd Summer Conference, Prague, 8-11 September, 1997.

[46] ROY M.F., Basic algorithms in real algebraic geometry and their complexity : from Sturm's theorem to the existential theory of reals, *Lectures in Real Geometry, Ed. : Fabrizio Broglia*, 1-67, Walter de Gruyter & Co., Berlin.

[47] SAINSAULIEU L., Finite Volume Approximation of Two-Phase Fluid Flows Based on an Approximate Roe-type Riemann Solver, J. Comput. Phys., 121, 1-28, 1995.

[48] SAUREL R. and ABGRALL R., A Method for Compressible Multiphase Flows with Interfaces, Proc. ICMF'98, Third International Conference on Multi-Phase Flow, June 8-12, 1998, Lyon, France.

[49] STÄDTKE H. and HOLTBECKER R., Hyperbolic Model for Inhomogeneous Two-Phase Flow, Proc. Int. Conf. On Multiphase Flows, September 24-27, 1991, University of Tsukuba, Japan.

[50] STÄDTKE H., FRANCHELLO G. and WORTH B., Numerical Simulation of Multi-Dimensional Two-Phase Flow Based on Flux Vector Splitting, Nucl. Eng. Design, 177, 199-213, 1997.

[51] STEWART H.B., WENDROFF B., Two-phase flows : models and methods, *J. Comput. Phys.*, 1984, **56**, 363-409.

[52] TAJCHMAN M. and FREYDIER P., *Méthode Volumes Finis Flux Caractéristiques. Application un calcul bidimensionnel sur un maillage non conforme*, Note, Département Transferts Thermiques et Aérodynamique, Direction des Etudes et Recherches, Electricité de France, EDF HT-30/96/004/A, May 1996.

[53] TORO E.F., Riemann-Problem Based Techniques for Computing Reactive Two-Phase Flows, in *Numerical Combustion*, A. Dervieux and B. Larrouturou, Eds., Lect. Notes in Physics, 351, 472, Springer-Verlag, 1989.

[54] TOUMI I., A weak formulation of Roe's approximate Riemann solver , J. Comput. Phys. 102 (1992), 360-373.

[55] TOUMI I., An upwind numerical method for a six equation two-fluid model, Nuclear Science and Engineering, 123, 147-168 (1996).

[56] VAN LEER B., Flux Vector Splitting for the Euler Equations, ICASE Technical Report, No. 82-30, 1982.

[57] VAN LEER B., Towards the ultimate conservative difference scheme IV: a new approach to numerical convection, J. Comp. Phys. 23 (1977), pp; 276-279.